Title

Perturbation of the O-U-O Angle in Uranyl by Coordination to a 12-Membered Macrocycle

Journal

INORGANIC CHEMISTRY, 55(11)

ISSN

0020-1669

Authors

Pedrick, EA
Schultz, JW
Wu, G
et al.

Publication Date

2016-06-06

DOI

10.1021/acs.inorgchem.6b00799

Peer reviewed

Perturbation of the O-U-O Angle in Uranyl by Coordination to a 12-membered Macrocycle

Elizabeth A. Pedrick,[1] Jason W. Schultz,[2] Guang Wu,[1] Liviu M. Mirica,[2] and Trevor W. Hayton*,[1]

1. Department of Chemistry and Biochemistry, University of California Santa Barbara, Santa Barbara, CA 93106

2. Department of Chemistry, Washington University in St. Louis, St. Louis, MO 63130

*To whom correspondence should be addressed. Email: hayton@chem.ucsb.edu

Abstract

Reaction of $[UO_2Cl_2(THF)_2]_2$ with 2 equiv of ^{H}N4 (^{H}N4 = 2,11-diaza[3,3](2,6) pyridinophane) or ^{Me}N4 (^{Me}N4 = *N,N'*-dimethyl-2,11-diaza[3,3](2,6) pyridinophane), in MeCN, results in the formation of $UO_2Cl_2(^{R}N4)$ (R = H; **1**; Me, **2**), which were isolated as yellow-orange solids in good yields. Similarly, reaction of $UO_2(OTf)_2(THF)_3$ with ^{H}N4 in MeCN results in the formation of $UO_2(OTf)_2(^{H}N4)$ (**3**), as an orange powder in 76% yield. Finally, reaction of $UO_2(OTf)_2(THF)_3$ with ^{Me}N4 in THF results in the formation of $[UO_2(OTf)(THF)(^{H}N4)][OTf]$ (**4**), as an orange powder in 73% yield. Complexes **1** – **4** have been fully characterized, including characterization by X-ray crystallography. These complexes exhibit the smallest O-U-O bond angles measured to date, ranging from 168.2(3)° (for **2**) to 161.7(5)° (for **4**), a consequence of an unfavorable steric interaction between the oxo ligands and the macrocycle backbone. A Raman spectroscopic study of **1**-**4** reveals no correlation between O-U-O angle and the U=O ν_{sym} mode. However, complex **1** and **2** do feature lower U=O ν_{sym} modes than complexes **3** and **4**, which can be rationalized by the stronger donor strength of Cl^- vs. OTf^-. This latter observation suggests that the identity of the equatorial ligands has a greater effect on the U=O ν_{sym} frequency than does a change in O-U-O angle, at least when the changes in the O-U-O angles are small.

Introduction

The uranyl ion, *trans*-UO_2^{2+}, is the most common fragment in uranium chemistry. It features short U=O bond lengths (ca. 1.78 Å),[1] and a *trans* arrangement of its two oxo ligands. Indeed, the O-U-O angle rarely deviates past 170°. This fixed stereochemistry has been rationalized by the presence of appreciable uranium $5f_z^3$ and $6p_z$ character within the O-U-O σ-bonding framework.[1,2] In contrast to the ubiquity of the *trans*-uranyl fragment, the *cis*-uranyl ion is unknown, and all attempts to synthesize a *cis*-uranyl complex have been unsuccessful thus far.[3-6] For example, reaction of $Cp^*_2UI(THF)$ with KC_8 and pyridine-*N*-oxide, in an attempt to generate *cis*-$Cp^*_2UO_2$, resulted in formation of the pentamethylcyclopentadienyl dimer and "uranium oxides" (Scheme 1a).[7] Similarly, reaction of Cp'_2UCl_2 (Cp' = 1,2,4-$C_5H_2{}^tBu_3$) with pyridine-*N*-oxide and KC_8 afforded a mixed-valent uranium oxo cluster (Scheme 1b).[8] Clark and co-workers attempted to enforce *cis*-oxo stereochemistry by ligating a tripodal ligand to the uranyl framework. However, reaction of $[Li]_3[N(CH_2CH_2NSi^tBuMe_2)_3]$ with $[K(18\text{-crown-}6)]_2[UO_2Cl_4]$ only resulted in formation of a mixed-valent U(V/VI) oxo-imido dimer, $[K(18\text{-crown-}6)(Et_2O)][UO(\mu_2\text{-}NCH_2CH_2N(CH_2CH_2NSi^tBuMe_2)_2)]_2$ (Scheme 1c).[3] In these three examples, the formation of the desired *cis*-oxo complex was thwarted by either ligand oxidation or ligand decomposition, and suggests that the successful isolation of *cis*-uranyl will require the use of a robust, redox-inactive co-ligand.

While a *cis*-uranyl complex remains elusive, several *cis*-bis(imido) complexes are known, including *cis*-$Cp^*_2U(NPh)_2$ and *cis*-$Cp_2U(N^tBu)_2$.[4,9,10] Their higher stability, relative to the unobserved oxo analogue, is probably due to a greater reliance on π-bonding within the $[U(NR)_2]^{2+}$ fragment, which diminishes the importance of the 6p orbital participation in the σ-bonding framework.[11] Similarly, Arnold and co-workers recently reported the isolation of

$[K]_2[(OUO)_2(L)]$ (L = polypyrrole macrocycle), which is formally generated by coupling of a *trans*-$[U^VO_2]^+$ fragment with a *cis*-$[U^VO_2]^+$ fragment within the binding pocket of the polypyrrole macrocycle.[12,13] In this case, reduction of both uranium ions to U(V) likely lowers the energy penalty required for *cis*/*trans* isomerization. In this regard, oxidation of this complex with pyridine-*N*-oxide results in rearrangement of the *cis*-di(oxo) fragment back to the original *trans* structure. Consistent with this result, density functional theory (DFT) studies of $[UO_2(OH)_4]^{2-}$ reveal that the *cis* isomer is 18-20 kcal/mol higher in energy than the *trans* isomer, depending on the method used.[14,15] Similarly, calculations reveal that the *cis* isomer of $[UO_2(N(SiH_3)_2)_3]^-$ is 31 kcal/mol less stable than the *trans* isomer.[16] These large destabilizations likely reflect the lack of an Inverse Trans Influence (ITI) in the *cis*-UO_2^{2+} fragment,[17-21] and further highlight the challenges inherent in isolating a *cis*-uranyl complex. Despite these challenges, though, there is still considerable interest in the synthesis of an authentic *cis*-uranyl complex, as this fragment would provide unique insights into actinide covalency and f orbital participation in bonding.[1]

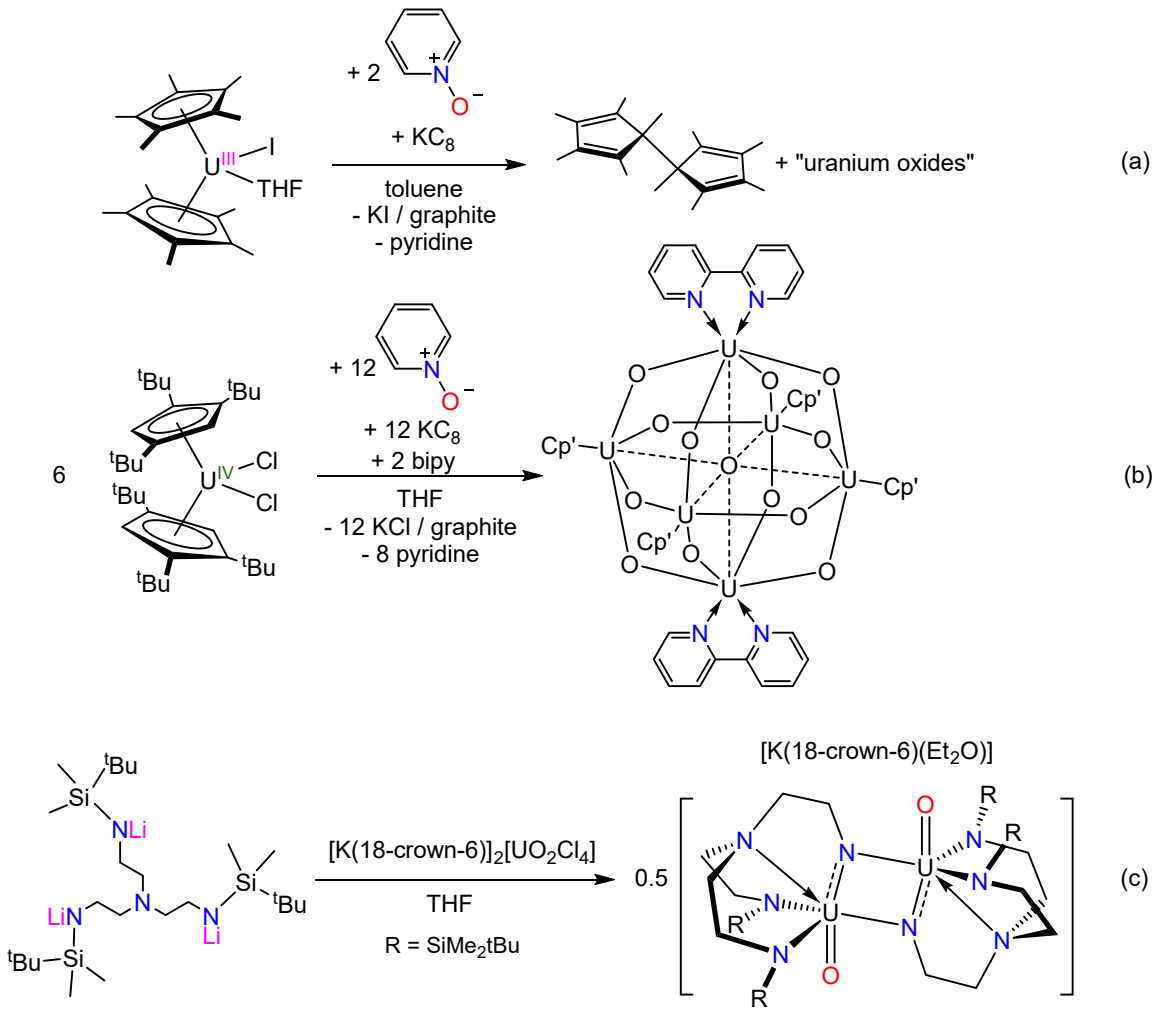

Scheme 1. Previous attempts to generate a *cis*-uranyl complex. Reaction (a) taken from Ref. [7]. Reaction (b) taken from Ref. [8]. Reaction (c) taken from Ref. [3].

Drawing inspiration from the results of Clark and co-workers, we sought to coordinate a polydentate ligand, specifically a macrocyclic ligand, to the uranyl fragment to effect a *trans* to *cis* isomerization of the oxo ligands. Several researchers have previously explored the coordination of macrocycles to the uranyl ion. For example, Sessler and co-workers have demonstrated that the uranyl ion can fit within the binding pocket of the 20-membered pentaphyrin ligand.[22] With this large binding pocket there is no steric pressure placed upon the two oxo ligands, and, as a result, the *trans* configuration is observed experimentally.[22-24]

In contrast, there are no known uranyl porphyrin complexes, likely because the uranyl ion cannot be accommodated by the binding pocket of the smaller 16-membered porphyrin core.[23] These observations suggest that coordination of uranyl to a small (≤16 member ring size) macrocycle could effect the desired *trans*/*cis* isomerization. Accordingly, we sought to explore the reactivity of the uranyl ion with the 12-membered macrocyclic ligands, ^{H}N4 (^{H}N4 = 2,11-diaza[3,3](2,6) pyridinophane) and ^{Me}N4 (^{Me}N4 = *N,N'*-dimethyl-2,11-diaza[3,3](2,6) pyridinophane), which were shown recently to act as tetradentate ligands for transition metal ions, while leaving two open coordination sites in a *cis* arrangement.[25-27]

Results and Discussion

Addition of 2 equiv of ^{H}N4 to $[UO_2Cl_2(THF)_2]_2$, in MeCN, results in the formation of a yellow-orange slurry, from which $UO_2Cl_2(^{H}N4)$ (**1**) can be isolated as a yellow crystalline solid in 66% yield (Scheme 2). Similarly, addition of 2 equiv of ^{Me}N4 to $[UO_2Cl_2(THF)_2]_2$, in MeCN, results in the formation of an orange-yellow slurry, from which $UO_2Cl_2(^{Me}N4)$ (**2**) can be isolated as a yellow–orange powder in 73% yield (Scheme 2).

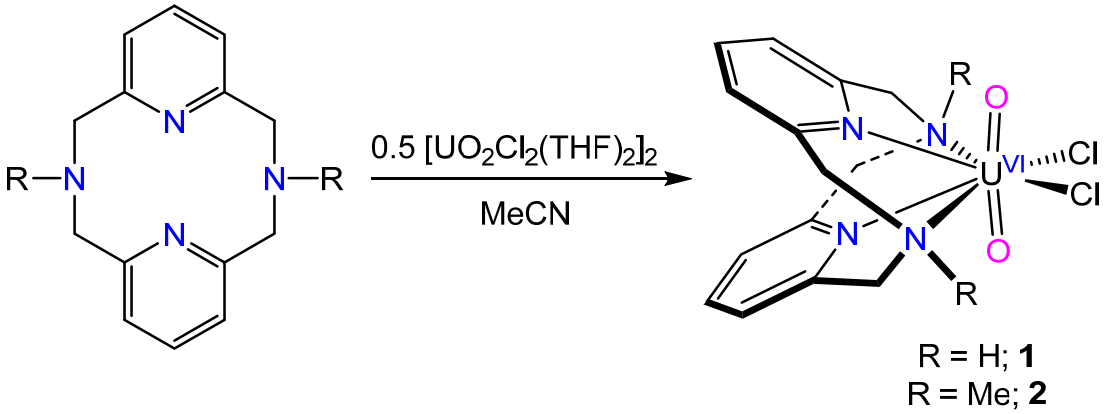

Scheme 2. Synthesis of complexes **1** and **2**.

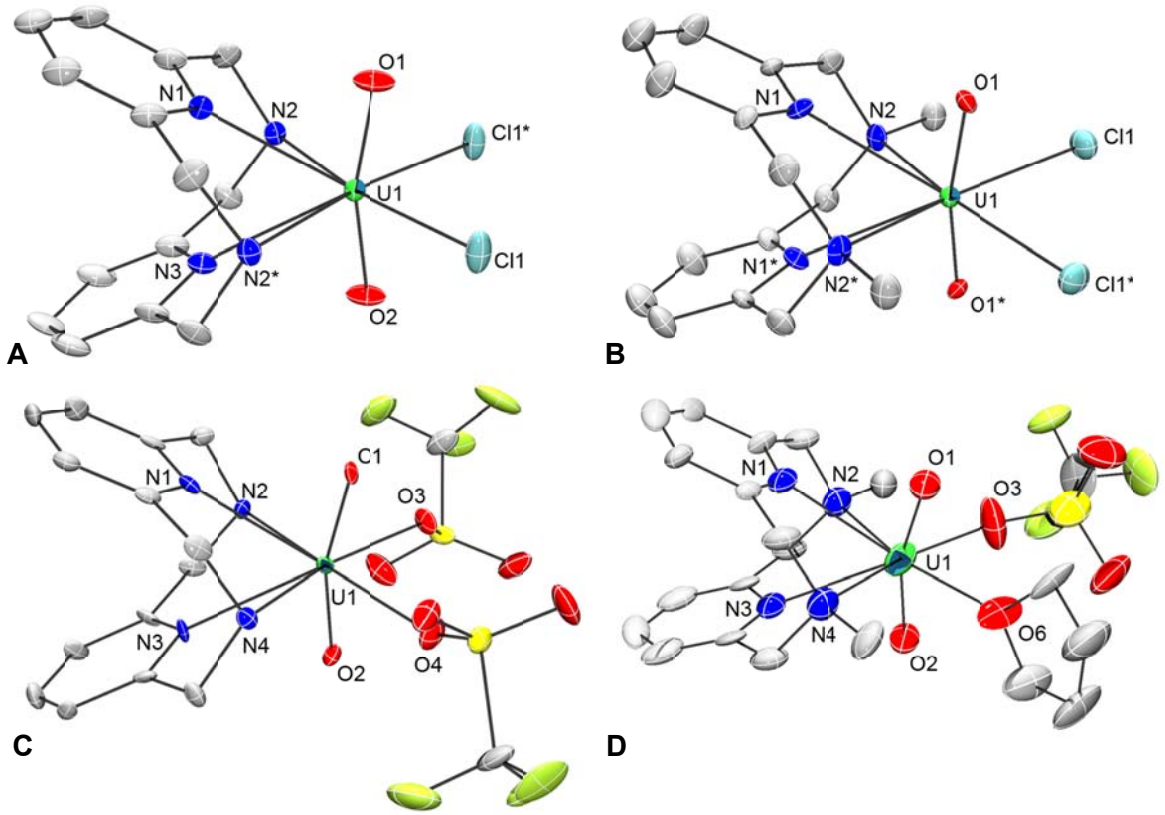

Figure 1. Solid-state structures of **1**-**4**, with 50% probability ellipsoids. A) Solid-state structure of $UO_2Cl_2(^{H}N4)\cdot 2MeCN$ (**1**·2MeCN). B) Solid-state structure of $UO_2Cl_2(^{Me}N4)\cdot 2MeCN$ (**2**·2MeCN). C) Solid-state structure of $UO_2(OTf)_2(^{H}N4)$ (**3**). D) Solid-state structure of $[UO_2(OTf)(THF)(^{Me}N4)][OTf]\cdot 0.5C_4H_8O$ (**4**·$0.5C_4H_8O$). Counterions, solvate molecules, and all hydrogen atoms have been omitted for clarity.

Complex **1** crystallizes in the monoclinic space group $P2_1/m$ as the MeCN solvate, **1**·2MeCN (Figure 1), while complex **2** crystallizes in the orthorhombic space group *C*mcm as the MeCN solvate, **2**·2MeCN (Figure 1). Complex **2** is also isolable in a second crystal modification (**2a**), which occupies the orthorhombic space group *P*bcn (See SI). Both **1** and **2** feature 8-coordinate geometries, with all four nitrogen atoms of the macrocyclic ligand coordinating to the U centers. The O-U-O angles in **1** and **2** are 164.1(3)° and 168.2(3)°,

respectively (Table 1). These O-U-O angles are amongst the smallest reported for the uranyl fragment, and are comparable to those observed for $Cp^*UO_2(^tBu\text{-}^{Mes}PDI^{Me})$ (O-U-O = 167.4(4)°),[28] $[NEt_4]_2[UO_2(\eta^5\text{-}Cp^*)(CN)_3]$ (O-U-O = 168.40(9)°),[29] $UO_2(SCS)(py)_2$ (SCS = $C(PPh_2S)_2$; O-U-O 168.5(1)°),[30] $[UO_2(BIPM^{TMS})(DMAP)_2]$ ($BIPM^{TMS}$ = $C(PPh_2NSiMe_3)_2$; DMAP = 4-(dimethylamino)pyridine; O-U-O = 167.16(9)°),[31] $[UO_2(O\text{-}2,6\text{-}^tBu_2C_6H_3)_2(THF)_2]$ (O-U-O = 167.8(4)°),[32] and $[UO_2(\kappa^2\text{-}NO_3)_2(^n Prbtp)]$ (^{n}Prbtp = 2,6-bis(5,6-di-*n*-propyl-1,2,4-triazin-3-yl)pyridine; O-U-O = 166.2(1)°).[33] We suggest that the deviation from linearity in complexes **1** and **2**, in particular, is due to an unfavorable steric interaction between the oxo ligands and the macrocycle backbone. In this regard, the smaller O-U-O angle in **1** vs. **2** may be due to the shorter $U\text{-}N_R$ (R = H, Me) and $U\text{-}N_{pyr}$ bond lengths in the former, which is a result of the smaller steric profile of ^{H}N4 vs. ^{Me}N4. A difference in $M\text{-}N_R$ bond distances between ^{H}N4 and ^{Me}N4 can also be seen in $[FeCl_2(^{H}N4)][Cl]$ (Fe-N = 2.189(1) Å),[34] and $[FeCl_2(^{Me}N4)][FeCl_4]$ (Fe-N = 2.237(2) and 2.219(2) Å).[35] The U-O bond lengths in **1** (1.776(5) and 1.785(5) Å) and **2** (1.779(6) Å), in contrast to the O-U-O angles, are similar to those exhibited by *trans*-uranyl.[33] Interestingly, the $N_{pyr}\text{-}M\text{-}N_{pyr}$ angles in **1** (58.5(2)°) and **2** (56.2(2)°) are much smaller than those observed in other ^{H}N4 and ^{Me}N4 complexes,[36-38] such as $[Fe(^{H}N4)Cl_2][Cl]$ (84.95(7)°),[34] $[FeCl_2(^{Me}N4)][FeCl_4]$ (78.05(8)°),[35] $OsCl_2(^{Me}N4)$ (82.4(3)°),[39] and $MnCl_2(^{Me}N4)$ (73.5(1)°).[40] This difference can be rationalized by greater steric constraints placed upon the ^{R}N4 ligands by the uranyl fragment in complexes **1** and **2**.

Table 1. Selected bond lengths (Å) and angles (deg) for complexes **1**-**4**.

	1	**2**	**2a**	**3**	**4**
U=O	1.776(5) 1.785(5)	1.779(6)	1.769(4)	1.759(6) 1.781(6)	1.76(1) 1.77(1)
$U\text{-}N_{pyr}$	2.639(6) 2.674(7)	2.732(5)	2.693(5)	2.626(7) 2.635(7)	2.68(1) 2.73(1)
$U\text{-}N_R$	2.601(5)	2.727(6)	2.728(5)	2.580(7) 2.597(7)	2.63(1) 2.67(1)
U-Cl	2.735(1)	2.686(2)	2.677(2)		

U-O_{OTf}				2.397(6) 2.409(6)	2.34(1)
O-U-O	164.1(3)	168.2(3)	168.3(3)	162.8(3)	161.7(5)
N_{pyr}-U-N_{pyr}	58.5(2)	56.2(2)	57.3(2)	59.4(2)	57.8(3)
Distance of the N_{pyr} atom from the equatorial plane	av. 1.298 Å	1.288(5) Å	1.083(5) Å	av. 1.302 Å	av. 1.305 Å

Another interesting aspect of these structures is the displacement of the N atoms of the two ^{R}N4 pyridine rings from the uranyl equatorial plane (defined by U1, N2, N2*, Cl1 and Cl1* in **1** and U1, N2, and N2* in **2**). In particular, the N_{pyr} atoms are displaced from the uranyl equatorial plane by 1.298 Å and 1.288(5) Å in **1** and **2**, respectively (Table 1). Deviations of multiple donor atoms from the equatorial plane of the UO_2^{2+} ion are very rare, and only a handful of examples are known.[33,41-45] For instance, the nitrogen atoms in $[UO_2(terpy)_2][OTf]_2$ (terpy = 2,6-bis(2-pyridyl)pyridine) and $[UO_2(phen)_3][OTf]_2$ (phen = 1,10-phenanthroline), feature maximum displacements from the uranyl equatorial plane of 0.49 and 0.71 Å, respectively.[43,46] Similarly, an N atom in the recently reported $UO_2Cl_2(H_2BBP)$ (H_2BBP = 2,6-bis(2-benzimidazolyl)pyridine) is displaced from the uranyl equatorial plane by 0.74 Å.[41] The most striking example of donor atom displacement from the equatorial plane is that exhibited by $[NEt_4]_2[UO_2(\eta^5\text{-}Cp^*)(CN)_3]$. In this example, the maximum displacement of one of the carbon atoms on the cyclopentadienyl ring is 1.494(6) Å.[29]

In an effort to strengthen (and shorten) the U-N bonds, and thereby decrease the O-U-O angle even further, we explored the substitution of the chloride ligands in **1** and **2** with weaker electron donating pseudo-halide ligands. Thus, addition of 1 equiv of ^{H}N4 to $UO_2(OTf)_2(THF)_3$ in MeCN, results in formation of an orange solution, from which $UO_2(OTf)_2(^{H}N4)$ (**3**) can be isolated in a 76% yield as an orange powder (Scheme 3).

Similarly, addition of 1 equiv of ^{Me}N4 to $UO_2(OTf)_2(THF)_3$ in THF, results in formation of $[UO_2(OTf)(THF)(^{Me}N4)][OTf]$ (**4**), which can be isolated as an orange powder in a 73% yield (Scheme 3). We also attempted the reaction of ^{Me}N4 and $UO_2(OTf)_2(THF)_3$ in MeCN. However, X-ray quality crystals could not be grown from this solvent.

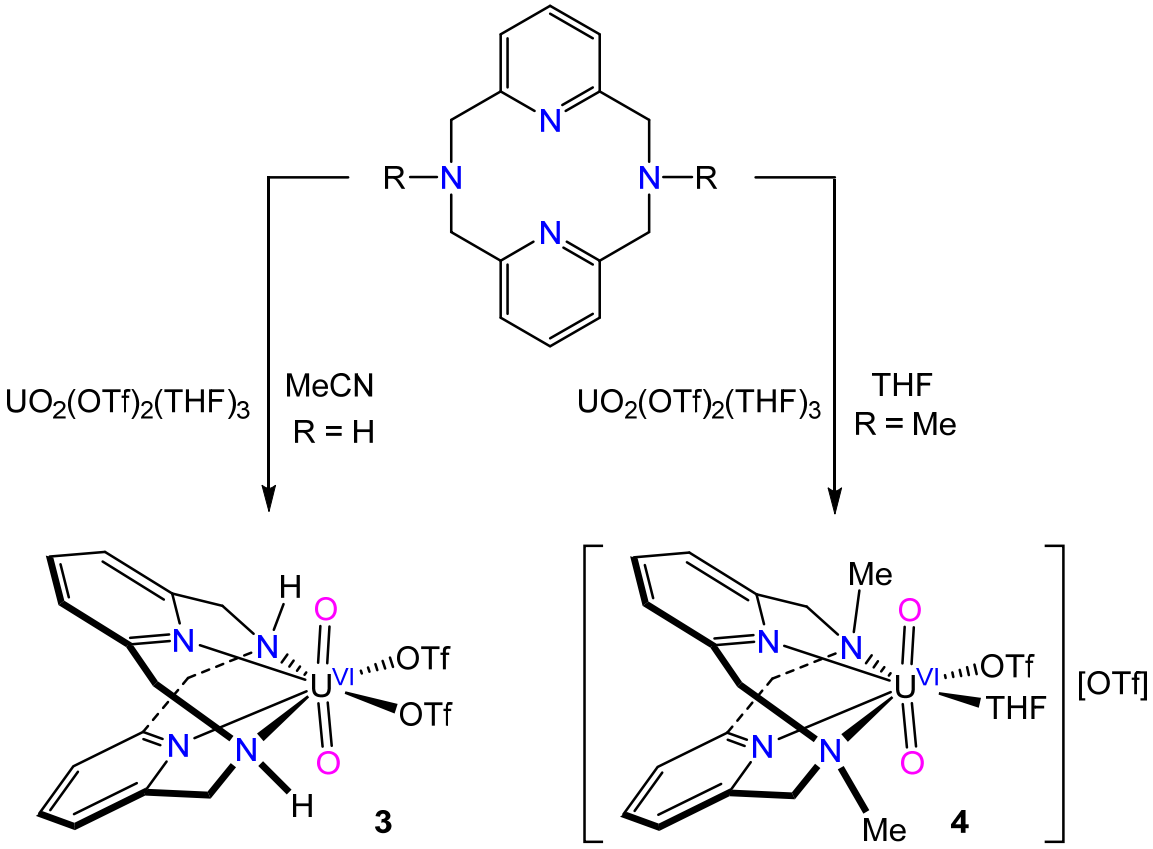

Scheme 3. Synthesis of complexes **3** and **4**.

Complex **3** crystallizes in the orthorhombic space group *P*na2$_1$, while complex **4** crystallizes in the triclinic space group *P*-1 as a THF solvate, **4**·0.5C_4H_8O (Figure 1). As with complexes **1** and **2**, all four nitrogen atoms of the macrocyclic ligand are coordinated to the U centers in **3** and **4**. Complex **3** also features two $[OTf]^-$ ligands within its inner coordination sphere, while complex **4** features a THF ligand and an $[OTf]^-$ ligand within its inner coordination sphere. Gratifyingly, the O-U-O bond angles in **3** (162.8(3)°) and **4**

(161.7(5)°) are smaller than those observed in **1** and **2** (Table 1), and, more significantly, are smaller than any O-U-O angles reported previously.[29-33] These smaller angles are likely due to the exchange of chloride for the poorly electron donating $[OTf]^-$ ligands, which strengthens the U-N interactions. That said, the U-N_R and U-N_{pyr} distances in **3** and **4** are not significantly shorter than those observed in **1** and **2**. Similar to **1** and **2**, both complexes exhibit U=O distances that are typical of the uranyl fragment (**3**: 1.759(6) and 1.781(6) Å, **4:** 1.76(1) and 1.77(1) Å).[47] The other metrical parameters in **3** and **4**, including the N_{pyr}-U-N_{pyr} angles, are comparable to those observed in **1** and **2**.

In an effort to better understand the effect of coordinating the ^{R}N4 macrocycles to the uranyl fragment we turned to Raman spectroscopy. This technique has proven to be useful for probing the relative strengths of the U=O bond in the uranyl fragment.[48] Raman spectroscopic data for complexes **1** – **4** are shown in Table 2. Complexes **1** and **2** exhibit U=O ν_{sym} modes at 813 and 815 cm^{-1}, respectively, in their Raman spectra. Interestingly, these values are on the lower end of the U=O ν_{sym} modes measured previously for the uranyl ion, and are similar to those observed for uranyl complexes with anionic, electron rich ligands, such as $[UO_2(CO_3)_3]^{4-}$ and $UO_2(^{Ar}acnac)_2$ (^{Ar}acnac = Ar*N*C(Ph)CHC(Ph)*O*; Ar = 3,5-$^tBu_2C_6H_3$).[49,50] For further comparison, the U=O ν_{sym} mode in $[UO_2Cl_2(THF)_2]_2$ was found to be 20 cm^{-1} higher, at 835 cm^{-1}. Both of these observations suggest that coordination of the macrocycle ligand to the uranyl ion does weaken the U-O bond to some extent. Complexes **3** and **4** exhibit U=O ν_{sym} modes at 833 and 831 cm^{-1}, respectively (Table 2), in their Raman spectra. For comparison, the U=O ν_{sym} mode in $UO_2(OTf)_2(THF)_3$ is observed at 842 cm^{-1}, an increase of ca. 10 cm^{-1} vs. the values observed for **3** and **4**. Again, this difference can be interpreted as evidence that the U=O bonds in the uranyl moiety are weakened upon coordination of the ^{R}N4 macrocycle. That said, it is unlikely that the decrease in the U=O ν_{sym} mode observed upon coordination of ^{R}N4 to $[UO_2Cl_2(THF)_2]_2$ or $UO_2(OTf)_2(THF)_3$ is due

to the bending of the O-U-O fragment. Instead, this decrease is probably due to coordination of a relatively good tetradentate donor to the uranyl moiety. In particular, it should be noted that complexes **1** and **2**, which feature larger O-U-O angles than **3** and **4**, actually exhibit weaker U=O bonds (as indicated by their lower U=O ν_{sym} modes). Their weaker U=O bonds can be rationalized by the stronger donor strength of Cl^- vs. OTf^-, highlighting the fact that the identity of the equatorial ligands has a greater effect on the U=O ν_{sym} frequency than does a change in O-U-O angle, at least when the changes in the O-U-O angles are small.

Table 2. Comparison of the U=O ν_{sym} Stretching Frequency for a Series of Uranyl Complexes.

Complex	**U=O ν_{sym} stretch (cm^{-1})**	**Reference**
$[UO_2(OH)_4]^{2-}$	784	51
$Cp^*UO_2(^tBu\text{-}^{Mes}PDI^{Me})$	789	28
$UO_2(OAr)_2(THF)_2$ (Ar = 2,6-$Ph_2C_6H_3$)	808	48
$[UO_2(CO_3)_3]^{4-}$	812	49
$UO_2(^{Ar}acnac)_2$ ($^{Ar}acnac$ = Ar*N*C(Ph)CHC(Ph)*O*; Ar = 3,5-$^tBu_2C_6H_3$)	812	50
$UO_2Cl_2(^{H}N4)$ (**1**)	813	this work
$UO_2Cl_2(^{Me}N4)$ (**2**)	815	this work
$UO_2(^{tBu}acnac)_2(THF)$ ($^{tBu}acnac$ = ^{t}Bu*N*C(Ph)CHC(Ph)*O*)	823	50
$UO_2(dbm)_2(THF)$ (dbm = *O*C(Ph)CHC(Ph)*O*)	823	21
$[UO_2(OTf)(THF)(^{Me}N4)][OTf]$ (**4**)	831	this work
$UO_2(OTf)_2(^{H}N4)$ (**3**)	833	this work
$[UO_2Cl_2(THF)_2]_2$	835	this work
$[UO_2(Ph_3PO)_4][OTf_2]$	839	52
$UO_2(OTf)_2(THF)_3$	842	this work
$[UO_2(OAc)_3]^-$	843	49
$[UO_2(dppmo)_2OTf][OTf]$ (dppmo = $Ph_2P(O)CH_2P(O)Ph_2$)	849	53
$[UO_2Cl_4]^{2-}$	854	49
$[UO_2(H_2O)_5]^{2+}$	870	49

Finally, we explored the chemical properties and solution phase behavior of complexes **1** – **4**. Complexes **1** – **3** are insoluble in non-polar solvents, aromatic solvents,

and Et_2O and THF, and only sparingly soluble in CH_2Cl_2 and MeCN. In contrast, complex **4** is somewhat soluble in THF, and very soluble in CH_2Cl_2 and MeCN. The ^1H NMR spectrum of **1** in CD_2Cl_2 features diastereotopic methylene environments at 5.23 ppm and 4.82 ppm for the ^{H}N4 ligand, consistent with its ligation to a metal center (Figure S9).[54-56] Similarly, the ^1H NMR spectrum of **2** in CD_2Cl_2 exhibits diastereotopic methylene resonances at 4.85 and 4.29 ppm for the ^{Me}N4 ligand (Figure S11). Also observed in this spectrum is a singlet at 3.57 ppm, which is assignable to the two methyl substituents. The ^1H NMR spectrum of **3** in CD_2Cl_2 features diastereotopic methylene environments at 5.19 ppm and 4.91 ppm for the ^{H}N4 ligand (Figure S13).[54] In addition, this spectrum also features a broad resonance at 5.76 ppm, which we have assigned to the NH substituent. The $^{19}F\{^1H\}$ NMR spectrum of **3** exhibits a singlet -77.41 ppm. As observed for **3**, the ^1H NMR spectrum of **4** in CD_2Cl_2 exhibits diastereotopic methylene resonances at 4.87 and 4.53 ppm (Figure S17). The spectrum also features a CH_3 resonance at 3.59 ppm and two broad singlets at 3.73 and 1.84 ppm, which are assignable to the THF ligand. The $^{19}F\{^1H\}$ NMR spectrum of **4** in CD_2Cl_2 only exhibits a single resonance at -77.56 ppm, suggesting that the inner- and outer-sphere $[OTf]^-$ moieties undergo rapid exchange in solution.

Complexes **1** – **4** are also quite soluble in pyridine. However, dissolution of complex **2** in pyridine-d_5 results in displacement of the macrocycle from the uranyl coordination sphere, according to ^1H NMR spectroscopy, along with probable formation of $UO_2(py)_3(Cl)_2$ (eq 1).[57] This observation is significant because it suggests that uranyl-macrocycle interaction in **2** is relatively weak; no doubt because of the mismatch between the uranyl ion and the ^{Me}N4 macrocycle binding pocket. Dissolution of **1**, **3**, or **4** in pyridine does not result in macrocycle dissociation, likely because of the smaller steric profile of ^{H}N4 (in the case of **1** and **3**) or the positive charge of the complex (in the case of **4**). Both effects are anticipated to strengthen the uranyl–macrocycle bonds.

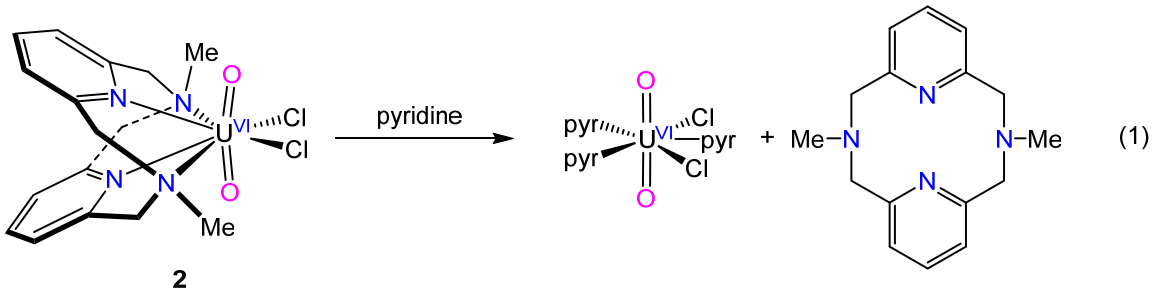

2 (1)

Conclusion

Ligation of the 12-membered macrocyclic ligands ^{H}N4 and ^{Me}N4 to the uranyl ion results in the formation of the 8-coordinate complexes $UO_2Cl_2(^{R}N4)$ (R = H; **1**; Me, **2**), $UO_2(OTf)_2(^{H}N4)$ (**3**), and $[UO_2(OTf)(THF)(^{Me}N4)][OTf]$ (**4**). All four complexes feature O-U-O angles that are 168° or smaller. Complexes **3** and **4**, in particular, exhibit the smallest O-U-O angles yet reported. These small O-U-O angles are a result of steric repulsion between the oxo ligands of the uranyl fragment and the macrocycle backbone, which is a consequence of the small binding pocket of the ^{R}N4 ligand. Perhaps more importantly, our results reveal that coordination of a small macrocycle to the uranyl ion is a viable strategy for the perturbation of the O-U-O angle. While coordination of ^{H}N4 and ^{Me}N4 to the uranyl ion did not result in *trans*/*cis* isomerization, as intended, our results do give some insight into new strategies for the generation of a *cis*-uranyl complex. For one, the relatively small N_{pyr}-U-N_{pyr} angles extant in complexes **1** – **4** reveal that the ^{R}N4 macrocycles still feature significant flexibility. As a result, we suggest that future studies focus on macrocycles with even greater rigidity, such as the "cross-bridged" cyclam ligands.[58,59] Secondly, the coordination of an anionic macrocyclic ligand to uranyl, which would result in even shorter uranyl-macrocycle bonds on account of the greater electrostatic attraction to UO_2^{2+}, should also better promote the desired *trans*/*cis* isomerization.

Experimental

General. All reactions and subsequent manipulations were performed under anaerobic and anhydrous conditions under an atmosphere of nitrogen. Et_2O, THF and toluene were dried by passage over activated molecular sieves using a Vacuum Atmospheres solvent purification system. CH_2Cl_2, CD_2Cl_2, MeCN, MeCN-d_3 and pyr-d_5 were dried over activated 3Å molecular sieves for 24 h before use. $[UO_2Cl_2(THF)_2]_2$,[47] $UO_2(OTf)_2(THF)_3$,[60] ^{H}N4,[61] and ^{Me}N4,[62] were prepared according to literature procedures. All other reagents were purchased from commercial suppliers and used as received.

NMR spectra were recorded on a Varian UNITY INOVA 400 spectrometer or a Varian UNITY INOVA 500 spectrometer. ^{1}H NMR spectra were referenced to external $SiMe_4$ using the residual protio solvent peaks as internal standards. The chemical shifts of ^{19}F{^{1}H} were referenced indirectly with the ^{1}H resonance of $SiMe_4$ at 0 ppm, according to IUPAC standard.[63,64] IR spectra were recorded on a Mattson Genesis FTIR/Raman spectrometer. UV-vis/NIR experiments were performed on a UV-3600 Shimadzu spectrophotometer. Elemental analyses were performed by the Microanalytical Laboratory at UC Berkeley.

Raman Spectroscopy. Raman spectra were recorded on a LabRam Aramis microRaman system (Horiba Jobin Yvon) equipped with 1200 grooves/mm holographic gratings, and Peltier-cooled CCD camera. The 633 nm output of a Melles Griot He-Ne laser was used to excite the sample, and spectra were collected in a back scattering geometry using a confocal Raman Microscope (high stability BX40) equipped with Olympus objectives (MPlan 50x). Sample preparation was performed inside the glovebox: Pure crystalline solid samples were placed between a glass microscope slide and coverslip, sealed with a bead of silicone grease, and removed from the glovebox for spectral acquisition.

X-ray Crystallography. The solid-state molecular structures of complexes **1** – **4** were

determined similarly with exceptions noted in the following paragraph. Crystals were mounted on a cryoloop under Paratone-N oil. Data collection was carried out on a Bruker KAPPA APEX II diffractometer equipped with an APEX II CCD detector using a TRIUMPH monochromater with a Mo Kα X-ray source (α = 0.71073 Å). Data for **1** - **4** were collected at 100(2) K, using an Oxford nitrogen gas cryostream system. A hemisphere of data was collected using ω scans with 0.5° frame widths. Frame exposures of 5, 10, 15, 5, and 45 seconds were used for complexes **1**, **2**, **2a**, **3**, and **4**, respectively. Data collection and cell parameter determination were conducted using the SMART program.[65] Integration of the data frames and final cell parameter refinement were performed using SAINT software.[66] Absorption correction of the data was carried out using the multi-scan method SADABS.[67] Subsequent calculations were carried out using SHELXTL.[68] Structure determination was done using direct or Patterson methods and difference Fourier techniques. All hydrogen atom positions were idealized, and rode on the atom of attachment. However, hydrogen atoms were not assigned to the disordered carbon atoms. Structure solution, refinement, graphics, and creation of publication materials were performed using SHELXTL.[68]

Complex **1** contains a MeCN solvent molecule that exhibits mild positional disorder about the methyl carbon atom. The positional disorder was addressed by modeling the CH_3 group in two orientations in a 50:50 ratio. Hydrogen atoms were not assigned to this carbon atom. Complex **1** was also mildly twined. The twinning was subsequently revealed by using the program CELL_NOW.[69] Complex **2** contains two oxo ligands and two chloride ligands in the main residue that exhibit positional disorder. The positional disorder was addressed by modeling the affected atoms in two orientations in a 50:50 ratio. Additionally, complex **2** exhibits some mild positional disorder of the two MeCN solvent molecules. Hydrogen atoms were not assigned to these carbon atoms. Complex **4** exhibits positional disorder of one OTf moiety in the main residue. This disorder was addressed by modeling the OTf moiety in two

orientations in a 50:50 ratio. The atoms of the OTf moiety were not refined anisotropically. Complex **4** also contains a THF solvent molecule that exhibited positional disorder, which was address by modeling the molecule in two orientations in a 50:50 ratio. Disordered atoms were not refined anisotropically and were constrained with the EADP, DFIX, and FLAT commands. Hydrogen atoms were not assigned to these carbon atoms. A summary of relevant crystallographic data for **1 – 4** is presented in Table 3.

$[UO_2Cl_2(THF)_2]_2$. This complex was prepared according to the published procedure.[47] Raman (neat solid, cm^{-1}): 1491 (w), 1463 (w), 1460 (w), 1367 (w), 1248 (w), 1231 (w), 1046 (w), 922 (m), 884 (vs), 835 (vs, U=O ν_{sym}), 238 (m), 192 (m), 176 (m).

$UO_2(OTf)_2(THF)_3$. This complex was prepared according to the published procedure.[60] Raman (neat solid, cm^{-1}): 1448 (w), 1332 (w), 1233 (m), 1162 (w), 1029 (sh w), 1016 (m), 999 (sh w), 915 (m), 878 (m), 843 (s, U=O ν_{sym}), 758 (m), 580 (w), 564 (w), 346 (w), 343 (w), 317 (m), 177 (m).

$UO_2Cl_2(^{H}N4)$ (1). To a stirring yellow solution of $[UO_2Cl_2(THF)_2]_2$ (30.6 mg, 0.032 mmol) in MeCN (2 mL), was added dropwise an off-white slurry of ^{H}N4 (15.0 mg, 0.062 mmol) in MeCN (1 mL). This resulted in an immediate color change to dark yellow, concomitant with the deposition of yellow solid. The mixture was then allowed to stir at room temperature for 1 h, whereupon the slurry was heated to ca. 70 °C. After 5 min at 70 °C, most of the solid had dissolved, and the yellow-orange slurry was quickly filtered through a Celite column (2 cm × 0.5 cm) supported on glass wool. Storage of the yellow filtrate at -25 °C for 24 h resulted in the deposition of a yellow crystalline solid (24.1 mg, 66% yield). X-ray quality crystals of **1** were grown from a hot, concentrated MeCN solution that was allowed to cool slowly to room temperature. Anal. Calcd for $UCl_2N_4O_2C_{14}H_{16}$: C, 28.93; H, 2.77; N, 9.64. Found: C, 29.25; H, 2.42; N, 9.91. ^{1}H NMR (CD_2Cl_2, 25 °C, 500 MHz): δ 7.57 (t, J_{HH} = 8 Hz, 2H, aryl CH), 7.17 (d, J_{HH} = 8 Hz, 4H, aryl CH), 5.23 (dd, J_{HH} = 6 Hz, J_{HH} = 16 Hz, 4H, CH_2), 4.82 (d,

J_{HH} = 16 Hz, 4H, CH_2). The N*H* resonance was not observed. ^{1}H NMR (pyr-d_5, 25 °C, 400 MHz): δ 7.39 (t, J_{HH} = 8 Hz, 2H, aryl CH), 7.05 (d, J_{HH} = 8 Hz, 4H, aryl CH), 6.47 (t, J_{HH} = 6 Hz, 2H, NH), 5.33 (dd, J_{HH} = 6 Hz, J_{HH} = 16 Hz, 4H, CH_2), 4.82 (d, J_{HH} = 16 Hz, 4H, CH_2). IR (KBr pellet, cm^{-1}): 1606 (sh m), 1599 (s), 1583 (m), 1470 (m), 1443 (s), 1423 (sh m), 1379 (m), 1373 (sh w), 1311 (m), 1290 (w), 1255 (w), 1209 (w), 1155 (m), 1088 (m), 1061 (s), 1041 (s), 1010 (sh m), 997 (s), 949 (w), 910 (s), 903 (vs), 889 (vs), 816 (s), 791 (s), 752 (m), 706 (w), 671 (w), 636 (vs), 480 (w). Raman (neat solid, cm^{-1}): 1582 (w), 1395 (w), 1260 (w), 1099 (w), 1015 (m), 910 (w), 813 (vs, U=O ν_{sym}), 760 (w), 709 (w), 520 (w), 424 (w), 196 (m).

UO_2Cl_2(^{Me}N4) (2). To a stirring yellow solution of $[UO_2Cl_2(THF)_2]_2$ (48.5 mg, 0.050 mmol) in MeCN (1 mL), was added dropwise a colorless solution of ^{Me}N4 (24.3 mg, 0.091 mmol) in MeCN (1 mL). This resulted in an immediate color change to orange-yellow, concomitant with the deposition of an orange-yellow precipitate. This orange-yellow slurry was allowed to stir at room temperature for 10 min, whereupon the orange-yellow solid was isolated by decanting off the supernatant. The solid was washed with Et_2O (1 mL), and then dried *in vacuo* (41.8 mg, 73% yield). X-ray quality crystals of **2** were grown from a concentrated MeCN solution layered with and equal volume of Et_2O, which was stored at -25 °C for 24 h. Anal. Calcd for $UCl_2N_4O_2C_{16}H_{20}$: C, 31.54; H, 3.31; N, 9.20. Found: C, 31.17; H, 2.58; N, 10.35. ^{1}H NMR (CD_2Cl_2, 25 °C, 400 MHz): δ 7.52 (t, J_{HH} = 8 Hz, 2H, aryl CH), 7.05 (d, J_{HH} = 8 Hz, 4H, aryl CH), 4.85 (d, J_{HH} = 15 Hz, 4H, CH_2), 4.29 (d, J_{HH} = 15 Hz, 4H, CH_2), 3.57 (s, 6H, CH_3). IR (KBr pellet, cm^{-1}): 1597 (m), 1578 (w), 1468 (m), 1452 (sh m), 1446 (s), 1427 (sh w), 1385 (m), 1367 (w), 1309 (w), 1263 (w), 1254 (w), 1232 (w), 1219 (m), 1182 (w), 1165 (m), 1093 (sh w), 1088 (m), 1082 (m), 1014 (s), 980 (w), 951 (w), 895 (vs), 885 (sh m), 812 (sh w), 802 (s), 762 (m), 727 (w), 636 (w), 538 (w), 471 (w), 455 (w). Raman (neat solid, cm^{-1}): 1580 (w), 1465 (w), 1454 (w), 1386 (w), 1258 (w), 1085 (w), 1015 (m), 815 (s, U=O ν_{sym}),

769 (w), 730 (w), 403 (m), 396 (m), 284 (m), 240 (m), 199 (m), 152 (m), 118 (vs).

$UO_2(OTf)_2(^{H}N4)$ (3). To a stirring yellow solution of $UO_2(OTf)_2(THF)_3$ (49.5 mg, 0.063 mmol) in MeCN (1 mL), was added dropwise an off-white slurry of $^{H}N4$ (14.6 mg, 0.061 mmol) in MeCN (1 mL). This resulted in an immediate color change to orange. The orange solution was allowed to stir at room temperature for 10 min, whereupon it was filtered through a Celite column (2 cm × 0.5 cm) supported on glass wool. The resulting orange filtrate was concentrated *in vacuo* to ca. 1 mL, and layered with Et_2O (3 mL). Storage of this solution at -25 °C for 24 h resulted in the deposition of orange powder (38.6 mg, 76% yield). X-ray quality crystals were grown from a MeCN solution layered with an equal volume of Et_2O, which was stored at -25 °C for 24 h. Anal. Calcd for $UF_6N_4O_8S_2C_{16}H_{16}$: C, 23.77; H, 1.99; N, 6.93. Found: C, 24.19; H, 1.21; N, 7.09. ^{1}H NMR (CD_2Cl_2, 25 °C, 400 MHz): δ 7.66 (t, J_{HH} = 8 Hz, 2H, aryl CH), 7.29 (d, J_{HH} = 8 Hz, 4H, aryl CH), 5.76 (br s, 2H, N*H*), 5.19 (dd, J_{HH} = 5 Hz, J_{HH} = 16 Hz 4H, CH_2), 4.91 (d, J_{HH} = 16 Hz, 4H, CH_2). ^{1}H NMR (pyr-d_5, 25 °C, 400 MHz): δ 7.59 (br t, J_{HH} = 9 Hz, 2H, aryl CH), 7.28 (d, J_{HH} = 7 Hz, 4H, aryl CH), 6.17 (br s, 2H, N*H*), 5.23 (br d, J_{HH} = 14 Hz 4H, CH_2), 4.96 (d, J_{HH} = 16 Hz, 4H, CH_2). ^{19}F{^{1}H} NMR (CD_2Cl_2, 25 °C, 376 MHz): δ -77.41. ^{19}F{^{1}H} NMR (pyr-d_5, 25 °C, 376 MHz): δ -77.29. IR (KBr pellet, cm^{-1}): 1610 (sh w), 1603 (w), 1585 (w), 1475 (w), 1450 (m), 1325 (s), 1309 (sh m), 1296 (m), 1252 (sh m), 1232 (s), 1203 (s), 1198 (s), 1178 (s), 1171 (sh m), 1088 (w), 1068 (w), 1057 (m), 1026 (m), 1009 (vs), 950 (w), 942 (sh w), 903 (s), 825 (w), 802 (m), 796 (w), 756 (w), 633 (vs), 579 (w), 571 (w), 515 (m). Raman (neat solid, cm^{-1}): 1587 (w), 1474 (w), 1393 (w), 1264 (w), 1243 (w), 1079 (w), 1028 (m), 833 (s, U=O ν_{sym}), 762 (m), 585 (w), 574 (w), 415 (m), 349 (w), 325 (w), 181 (w).

$[UO_2(OTf)(THF)(^{Me}N4)][OTf]$ (4). To a stirring yellow solution of $UO_2(OTf)_2(THF)_3$ (67.1 mg, 0.086 mmol) in THF (1.5 mL), was added dropwise a colorless solution of $^{Me}N4$ (22.0 mg, 0.082 mmol) in THF (1 mL). This resulted in the immediate color change to orange. The

mixture was allowed to stir at room temperature for 10 min, whereupon it was filtered through a Celite column (2 cm × 0.5 cm) supported on glass wool. The resulting orange filtrate was then layered with Et_2O (1 mL). Storage of this solution at -25 °C for 24 h resulted in the deposition an orange powder, which was isolated by decanting off the supernatant (56.8 mg, 73% yield). X-ray quality crystals were grown in a 2 vial system, whereby a THF solution (3 mL) of **4** was transferred to a 4 mL scintillation vial that was placed inside a 20 mL scintillation vial. Et_2O (2 mL) was then added to the outer vial. Storage of this 2 vial system at -25 °C for 24 h afforded orange X-ray quality crystals. Anal. Calcd for $UF_6N_4O_9S_2C_{22}H_{28}$: C, 29.08; H, 3.11; N, 6.17. Found: C, 29.50; H, 3.07; N, 5.89. ^{1}H NMR (CD_2Cl_2, 25 °C, 400 MHz): δ 7.67 (t, J_{HH} = 8Hz, 2H, aryl CH), 7.23 (d, J_{HH} = 8 Hz, 4H, aryl CH), 4.87 (d, J_{HH} = 15 Hz, 4H, CH_2), 4.53 (d, J_{HH} = 15 Hz, 4H, CH_2), 3.73 (br s, 4H, THF), 3.59 (br s, 6H, CH_3), 1.84 (br s, 4H, THF). ^{1}H NMR (pyr-d_5, 25 °C, 400 MHz): δ 7.59 (br s, 2H, aryl CH), 7.22 (br s, 4H, aryl CH), 4.94 (d, J_{HH} = 15 Hz, 4H, CH_2), 4.78 (d, J_{HH} = 16 Hz, 4H, CH_2), 3.66 (br s, 4H, THF), 2.93 (br s, 6H, CH_3), 1.62 (br s, 4H, THF). ^{19}F{^{1}H} NMR (CD_2Cl_2, 25 °C, 376 MHz): δ -77.57. ^{19}F{^{1}H} NMR (pyr-d_5, 25 °C, 376 MHz): δ -77.41. IR (KBr pellet, cm^{-1}): 3049 (w), 3006 (sh w), 2980 (m), 2962 (sh m), 2943 (sh m), 2877 (w), 2873 (w), 2806 (sh vw), 1603 (m), 1583 (m), 1470 (sh m), 1462 (m), 1452 (sh m), 1390 (w), 1362 (sh w), 1327 (s), 1265 (s), 1255 (s), 1234 (s), 1223 (m), 1205 (s), 1173 (sh m), 1155 (s), 1080 (sh w), 1068 (w), 1065 (w), 1030 (s), 1012 (s), 957 (w), 912 (m), 883 (m), 866 (m), 854 (m), 812 (m), 768 (m), 756 (w), 729 (w), 636 (vs), 580 (sh w), 573 (m), 526 (w), 517 (m), 471 (w). Raman (neat solid, cm^{-1}): 1608 (w), 1585 (w), 1465 (w), 1391 (w), 1262 (m), 1237 (w), 1227 (w), 1079 (w), 1030 (m), 1028 (m), 924 (w), 831 (s, U=O ν_{sym}), 766 (w), 764 (w), 574 (w), 418 (m), 347 (w), 187 (w), 116 (m).

Table 3. X-ray Crystallographic Information for 1-4

	1	**2**	**2a**
empirical formula	$UCl_2N_6O_2C_{18}H_{22}$	$UCl_2N_6O_2C_{20}H_{26}$	$UCl_2N_4O_2C_{16}H_{20}$
Crystal habit, color	block, yellow orange	shard, light yellow	block, orange
crystal size (mm)	0.15 × 0.15 × 0.05	0.1 × 0.05 × 0.025	0.1 × 0.1 × 0.05
crystal system	monoclinic	orthorhombic	orthorhombic
space group	$P2_1/m$	*C*mcm	*P*bcn
vol (Å^3)	1146.9(1)	2334(2)	1864.1(8)
a (Å)	8.3513(5)	16.085(7)	9.434(2)
b (Å)	15.0623(9)	10.152(4)	14.676(3)
c (Å)	9.9039(6)	14.291(6)	13.464(4)
α (deg)	90	90	90
β (deg)	112.981(3)	90	90
γ (deg)	90	90	90
Z	2	4	4
fw (g/mol)	660.32	691.40	609.29
density (calcd) (Mg/m^3)	1.912	1.968	2.171
abs coeff (mm^{-1})	7.334	7.213	9.011
F_{000}	622	1320	1144
Total no. reflections	2451	1285	1902
Unique reflections	2279	1149	1177
final R indices [I > 2σ(I)]	R_1 = 0.0286 wR_2 = 0.0764	R_1 = 0.0360 wR_2 = 0.0609	R_1 = 0.0304 wR_2 = 0.0510
largest diff peak and hole (e$^-$Å^{-3})	3.015 and -1.765	1.386 and -0.822	0.896 and -0.971
GOF	1.107	1.052	0.949

Table 3 (contd).

	3	**4**
empirical formula	$UF_6N_4O_8S_2C_{16}H_{16}$	$UF_6N_4O_9S_2C_{22}H_{28}$
Crystal habit, color	block, orange	rod, brown
crystal size (mm)	0.10 × 0.10 × 0.05	0.1 × 0.05 × 0.04
crystal system	orthorhombic	triclinic
space group	*P*na2_1	*P*-1
vol (Å^3)	2378.5(2)	3159(5)
a (Å)	11.7508(5)	12.33(1)
b (Å)	18.807(1)	16.38(2)
c (Å)	10.7623(4)	16.61(2)
α (deg)	90	90.59(2)
β (deg)	90	100.23(2)
γ (deg)	90	106.38(2)
Z	4	1
fw (g/mol)	808.48	3771.69
density (calcd) (Mg/m^3)	2.258	1.983
abs coeff (mm^{-1})	7.098	5.363
F_{000}	1528	1825

Total no. reflections	4744	10655
Unique reflections	3857	3616
final R indices [I > 2σ(I)]	R_1 = 0.0341 wR_2 = 0.0759	R_1 = 0.0612 wR_2 = 0.0812
largest diff peak and hole ($e^{-}Å^{-3}$)	1.771 and -2.114	1.344 and -1.170
GOF	0.930	0.823

Supporting Information

Crystallographic details (as CIF files) and spectral data for compounds **1** – **4**. This material is available free of charge via the Internet at http://pubs.acs.org.

Acknowledgements

This work was supported by the U.S. Department of Energy, Office of Basic Energy Sciences, Chemical Sciences, Biosciences, and Geosciences Division under Contract DE-SC-0001861 (to T.W.H.) and Contract DE-FG02-11ER16254 (to L.M.M.).

Notes

The authors declare no competing financial interest.

References

(1) Denning, R. G. *J. Phys. Chem. A* **2007**, *111*, 4125-4143.
(2) Cotton, S. *Lanthanide and Actinide Chemistry*; John Wiley & Sons, Ltd.: West Sussex, England, 2006.
(3) Duval, P. B.; Burns, C. J.; Buschmann, W. E.; Clark, D. L.; Morris, D. E.; Scott, B. L. *Inorg. Chem.* **2001**, *40*, 5491-5496.
(4) Arney, D. S. J.; Burns, C. J. *J. Am. Chem. Soc.* **1995**, *117*, 9448-9460.
(5) Villiers, C.; Thuéry, P.; Ephritikhine, M. *Angew. Chem. Int. Ed.* **2008**, *47*, 5892-5893.
(6) Vaughn, A. E.; Barnes, C. L.; Duval, P. B. *Angew. Chem. Int. Ed.* **2007**, *46*, 6622-6625.
(7) Cantat, T.; Graves, C. R.; Scott, B. L.; Kiplinger, J. L. *Angew. Chem. Int. Ed.* **2009**, *48*, 3681-3684.
(8) Duval, P. B.; Burns, C. J.; Clark, D. L.; Morris, D. E.; Scott, B. L.; Thompson, J. D.; Werkema, E. L.; Jia, L.; Andersen, R. A. *Angew. Chem. Int. Ed.* **2001**, *40*, 3357-3361.
(9) Arney, D. S. J.; Burns, C. J.; Smith, D. C. *J. Am. Chem. Soc.* **1992**, *114*, 10068-10069.
(10) Spencer, L. P.; Gdula, R. L.; Hayton, T. W.; Scott, B. L.; Boncella, J. M. *Chem. Commun.* **2008**, 4986-4988.
(11) Hayton, T. W.; Boncella, J. M.; Scott, B. L.; Batista, E. R.; Hay, P. J. *J. Am. Chem. Soc.* **2006**, *128*, 10549-10559.
(12) Arnold, P. L.; Jones, G. M.; Odoh, S. O.; Schreckenbach, G.; Magnani, N.; Love, J. B. *Nat. Chem.* **2012**, *4*, 221-227.
(13) Jones, G. M.; Arnold, P. L.; Love, J. B. *Angew. Chem. Int. Ed.* **2012**, *51*, 12584-12587.
(14) Schreckenbach, G.; Hay, P. J.; Martin, R. L. *Inorg. Chem.* **1998**, *37*, 4442-4451.
(15) Bühl, M.; Schreckenbach, G. *Inorganic Chemistry* **2010**, *49*, 3821-3827.
(16) Mullane, K. C.; Lewis, A. J.; Yin, H.; Carroll, P. J.; Schelter, E. J. *Inorg. Chem.* **2014**, *53*, 9129-9139.
(17) La Pierre, H. S.; Meyer, K. *Inorg. Chem.* **2013**, *52*, 529-539.
(18) Kovács, A.; Konings, R. J. M. *Chem. Phys. Chem.* **2006**, *7*, 455-462.
(19) Lam, O. P.; Franke, S. M.; Nakai, H.; Heinemann, F. W.; Hieringer, W.; Meyer, K. *Inorg. Chem.* **2012**, *51*, 6190-6199.
(20) Lewis, A. J.; Carroll, P. J.; Schelter, E. J. *J. Am. Chem. Soc.* **2013**, *135*, 511-518.
(21) Pedrick, E. A.; Wu, G.; Kaltsoyannis, N.; Hayton, T. W. *Chem. Sci.* **2014**, *5*, 3204-3213.
(22) Burrell, A. K.; Hemmi, G.; Lynch, V.; Sessler, J. L. *J. Am. Chem. Soc.* **1991**, *113*, 4690-4692.
(23) Sessler, J. L.; Vivian, A. E.; Seidel, D.; Burrell, A. K.; Hoehner, M.; Mody, T. D.; Gebauer, A.; Weghorn, S. J.; Lynch, V. *Coord. Chem. Rev.* **2001**, *216–217*, 411-434.
(24) Liao, M.-S.; Kar, T.; Scheiner, S. *J. Phys. Chem. A* **2004**, *108*, 3056-3063.
(25) Khusnutdinova, J. R.; Luo, J.; Rath, N. P.; Mirica, L. M. *Inorg. Chem.* **2013**, *52*, 3920-3932.
(26) Khusnutdinova, J. R.; Rath, N. P.; Mirica, L. M. *Inorg. Chem.* **2014**, *53*, 13112-13129.
(27) Zheng, B.; Tang, F.; Luo, J.; Schultz, J. W.; Rath, N. P.; Mirica, L. M. *J. Am. Chem. Soc.* **2014**, *136*, 6499-6504.
(28) Kiernicki, J. J.; Cladis, D. P.; Fanwick, P. E.; Zeller, M.; Bart, S. C. *J. Am. Chem. Soc.* **2015**, *137*, 11115-11125.

(29) Maynadie, J.; Berthet, J.-C.; Thuery, P.; Ephritikhine, M. *Chem. Commun.* **2007**, 486-488.
(30) Tourneux, J.-C.; Berthet, J.-C.; Cantat, T.; Thuery, P.; Mezailles, N.; Ephritikhine, M. *J. Am. Chem. Soc.* **2011**, *133*, 6162-6165.
(31) Lu, E.; Cooper, O. J.; McMaster, J.; Tuna, F.; McInnes, E. J. L.; Lewis, W.; Blake, A. J.; Liddle, S. T. *Angew. Chem. Int. Ed.* **2014**, *53*, 6696-6700.
(32) Wilkerson, M. P.; Burns, C. J.; Morris, D. E.; Paine, R. T.; Scott, B. L. *Inorg. Chem.* **2002**, *41*, 3110-3120.
(33) Berthet, J.-C.; Thuéry, P.; Dognon, J.-P.; Guillaneux, D.; Ephritikhine, M. *Inorg. Chem.* **2008**, *47*, 6850-6862.
(34) Raffard, N.; Carina, R.; Simaan, A. J.; Sainton, J.; Rivière, E.; Tchertanov, L.; Bourcier, S.; Bouchoux, G.; Delroisse, M.; Banse, F.; Girerd, J.-J. *Eur. J. Inorg. Chem.* **2001**, *2001*, 2249-2254.
(35) Chow, T. W.-S.; Wong, E. L.-M.; Guo, Z.; Liu, Y.; Huang, J.-S.; Che, C.-M. *J. Am. Chem. Soc.* **2010**, *132*, 13229-13239.
(36) O. Koch, W.; T. Kaiser, J. *Chem. Commun.* **1997**, 2237-2238.
(37) Koch, W. O.; Barbieri, A.; Grodzicki, M.; Schünemann, V.; Trautwein, A. X.; Krüger, H.-J. *Angew. Chem. Int. Ed.* **1996**, *35*, 422-424.
(38) Lee, W.-T.; Muñoz, S. B.; Dickie, D. A.; Smith, J. M. *Angew. Chem. Int. Ed.* **2014**, *53*, 9856-9859.
(39) Sugimoto, H.; Ashikari, K.; Itoh, S. *Inorg. Chem.* **2013**, *52*, 543-545.
(40) Albela, B.; Carina, R.; Policar, C.; Poussereau, S.; Cano, J.; Guilhem, J.; Tchertanov, L.; Blondin, G.; Delroisse, M.; Girerd, J.-J. *Inorg. Chem.* **2005**, *44*, 6959-6966.
(41) Copping, R.; Jeon, B.; Pemmaraju, C. D.; Wang, S.; Teat, S. J.; Janousch, M.; Tyliszczak, T.; Canning, A.; Grønbech-Jensen, N.; Prendergast, D.; Shuh, D. K. *Inorg. Chem.* **2014**, *53*, 2506-2515.
(42) Schettini, M. F.; Wu, G.; Hayton, T. W. *Inorg. Chem.* **2009**, *48*, 11799-11808.
(43) Berthet, J.-C.; Nierlich, M.; Ephritikhine, M. *Dalton Trans.* **2004**, 2814-2821.
(44) Sarsfield, M. J.; Steele, H.; Helliwell, M.; Teat, S. J. *Dalton Trans.* **2003**, 3443-3449.
(45) Sarsfield, M. J.; Helliwell, M.; Collison, D. *Chem. Commun.* **2002**, 2264-2265.
(46) Berthet, J.-C.; Nierlich, M.; Ephritikhine, M. *Chem. Commun.* **2003**, 1660-1661.
(47) Wilkerson, M. P.; Burns, C. J.; Paine, R. T.; Scott, B. L. *Inorg. Chem.* **1999**, *38*, 4156-4158.
(48) Fortier, S.; Hayton, T. W. *Coord. Chem. Rev.* **2010**, *254*, 197-214.
(49) Nguyen Trung, C.; Begun, G. M.; Palmer, D. A. *Inorg. Chem.* **1992**, *31*, 5280-5287.
(50) Brown, J. L.; Mokhtarzadeh, C. C.; Lever, J. M.; Wu, G.; Hayton, T. W. *Inorg. Chem.* **2011**, *50*, 5105-5112.
(51) Clark, D. L.; Conradson, S. D.; Donohoe, R. J.; Keogh, D. W.; Morris, D. E.; Palmer, P. D.; Rogers, R. D.; Tait, C. D. *Inorg. Chem.* **1999**, *38*, 1456-1466.
(52) Pedrick, E. A.; Wu, G.; Hayton, T. W. *Inorg. Chem.* **2015**, *54*, 7038-7044.
(53) Cornet, S. M.; May, I.; Redmond, M. P.; Selvage, A. J.; Sharrad, C. A.; Rosnel, O. *Polyhedron* **2009**, *28*, 363-369.
(54) Khusnutdinova, J. R.; Rath, N. P.; Mirica, L. M. *J. Am. Chem. Soc.* **2010**, *132*, 7303-7305.
(55) Tang, F.; Zhang, Y.; Rath, N. P.; Mirica, L. M. *Organometallics* **2012**, *31*, 6690-6696.
(56) Tang, F.; Qu, F.; Khusnutdinova, J. R.; Rath, N. P.; Mirica, L. M. *Dalton Trans.* **2012**, *41*, 14046-14050.
(57) Berthet, J.-C.; Siffredi, G.; Thuery, P.; Ephritikhine, M. *Dalton Trans.* **2009**, 3478-3494.
(58) Weisman, G. R.; Wong, E. H.; Hill, D. C.; Rogers, M. E.; Reed, D. P.; Calabrese, J. C. *Chem. Commun.* **1996**, 947-948.

(59) Wong, E. H.; Weisman, G. R.; Hill, D. C.; Reed, D. P.; Rogers, M. E.; Condon, J. S.; Fagan, M. A.; Calabrese, J. C.; Lam, K.-C.; Guzei, I. A.; Rheingold, A. L. *J. Am. Chem. Soc.* **2000**, *122*, 10561-10572.
(60) Oldham, S. M.; Scott, B. L.; Oldham, W. J. *Appl. Organometal. Chem.* **2006**, *20*, 39-43.
(61) Alpha, B.; Anklam, E.; Deschenaux, R.; Lehn, J.-M.; Pietraskiewiez, M. *Helv. Chim. Acta* **1988**, *71*, 1042-1052.
(62) Bottino, F.; Di Grazia, M.; Finocchiaro, P.; Fronczek, F. R.; Mamo, A.; Pappalardo, S. *J. Org. Chem.* **1988**, *53*, 3521-3529.
(63) Harris, R. K.; Becker, E. D.; Cabral De Menezes, S. M.; Goodfellow, R.; Granger, P. *Pure Appl. Chem.* **2001**, *73*, 1795-1818.
(64) Harris, R. K.; Becker, E. D.; Cabral De Menezes, S. M.; Granger, P.; Hoffman, R. E.; Zilm, K. W. *Pure Appl. Chem.* **2008**, *80*, 59-84.
(65) SMART Apex II, Version 2.1, Bruker AXS Inc., Madison, WI, 2005,
(66) SAINT Software User's Guide, Version 7.34a, Bruker AXS Inc., Madison, WI, 2005,
(67) SADABS, Sheldrick, G. M., University of Gottingen, Germany, 2005,
(68) SHELXTL PC, Version 6.12, Bruker AXS Inc., Madison, WI, 2005,
(69) CELL_NOW Version 2008-4, Sheldrick, G. M., Bruker AXS Inc., Madison, WI, 2008,

For Table of Contents Only

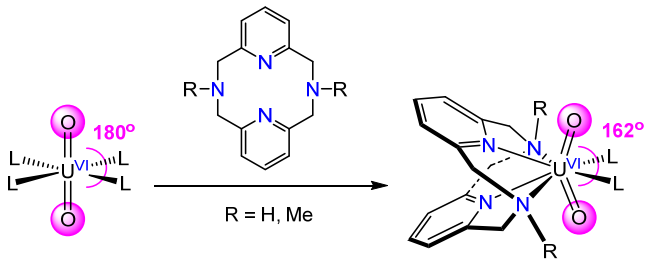

Addition of the 12-membered macrocycles, ^{H}N4 (^{H}N4 = 2,11-diaza[3,3](2,6) pyridinophane) or ^{Me}N4 (^{Me}N4 = *N,N'*-dimethyl-2,11-diaza[3,3](2,6) pyridinophane) to the uranyl fragment results in formation of 8-coordinate complexes, (^{R}N4)UO_2L_2. These complexes exhibit some of the smallest O-U-O bond angles yet reported.